NUMERICAL SIMULATION OF THREE-STEP HOT FORGING PROCESSES AND THEIR IMPACT ON THE MICROSTRUCTURE OF HIGH ENTROPY ALLOY

Michaela ŠTAMBORSKÁ, Tatiana PELACHOVÁ

Institute of Materials and Machine Mechanics, Slovak Academy of Sciences, Dúbravská cesta 9, 845 13 Bratislava, Slovak Republic, EU, michaela.stamborska@savba.sk

https://doi.org/10.37904/metal.2025.5142

Abstract

This study investigates the influence of F30-60-40 and F30-60-80 three-step hot forging processes on the microstructure of the $Al_{0.35}CoCrFeNi$ high entropy alloy. After forging, the alloy exhibited a single-phase face-centered cubic (FCC) structure. Numerical simulation of the hot forging processes was used to predict the evolution of grain formation. The simulation model was calibrated and validated using experimental compression data from the as-cast alloy, ensuring the accuracy of the model in predicting microstructural changes. During the third forging step F40 of the F30-60-40 process, a uniform distribution of dynamically recrystallized equiaxed grains with a median grain size of 64 ± 1 μm was observed. However, after the F30-60-80 forging process, dual grain size was observed in the sample, which could be attributed to the increased energy applied during the third forging step F80. The correlation between temperature, equivalent stress, equivalent plastic strain, and the resulting microstructure was analyzed. The simulations enabled the prediction of regions within the samples where dynamically recrystallized grains were formed. The study highlights the relationship between the forging process and the resulting microstructure and provides key information for optimizing the hot forging process to achieve desired material properties.

Keywords: High entropy alloy, hot forging, microstructure, numerical simulation, recrystallized grains

1. INTRODUCTION

High entropy alloys (HEAs) are a class of materials characterized by their complex composition of multiple principal elements, which results in unique properties such as excellent mechanical strength, corrosion resistance, resistance to anneal softening and high thermal stability [1, 2]. $Al_xCoCrFeNi$ is one of the most studied high entropy alloys, showing promising applications in extreme environments due to its superior properties [3]. However, the processing of these alloys to optimize their microstructure and mechanical properties remains a challenge, particularly during plastic deformation processes like hot forging [4, 5].

Hot forging is an important method for shaping metallic materials, and its effects on microstructure evolution, including grain size, recrystallization, and phase transformations, are critical in determining the material's final properties [4-6]. The process parameters such as temperature, strain rate, and forging steps significantly affect the microstructural properties of the alloy [7]. In particular, the formation of dynamically recrystallized grains and their distribution within the material plays a major role in determining the mechanical properties of high entropy alloys [8-11].

The subject of this article is to investigate the influence of F30-60-40 and F30-60-80 three-step hot forging processes on grain formation in $Al_{0.35}CoCrFeNi$ high entropy alloy and characterize the results of hot forging using finite element and microstructure analysis. The aim of this study is to understand the relationship between the forging parameters and the resulting microstructure, with a particular focus on grain formation, recrystallization dynamics, and the impact of increased energy during the final forging steps.

2. EXPERIMENTAL PROCEDURE

2.1 Casting and heat treatment

The studied $Al_{0.35}CoCrFeNi$ alloy was prepared from master alloys by induction melting in a vacuum induction furnace. The as-cast samples were cut transversally to smaller pieces using spark wire cutting machine. The cut samples with diameter of 23.8 mm and length of 65 mm were heat treated. The heat treatment (HT) consisted of solution annealing at a temperature of 1340 °C for 6 h under a protective argon atmosphere followed by a fan cooling to room temperature.

2.2 Forging process

Hot forging (HF) was carried out on a friction screw press FICEP PVX 160 machine, which uses supplied energy (up to 17000 J) to forge [11]. HT samples were pre-forged before HF by 25 % of the machine's energy which means kinetics energy of 4250 J at room temperature to slightly deform their cylindrical shape for better handling. Subsequently, HF process was applied to pre-forged samples which consisted of forging the samples in two three-step hot forging processes F30-60-40 and F30-60-80, as schematically shown in **Figure 1**. The samples were stabilization annealed for 20 minutes at the temperature of 1250 °C before each step of HF. At both forging processes, the samples were pressed with 30 % (F30) of the machine's energy at first, which corresponds kinetics energy of 5100 J. Subsequently, after the next stabilization annealing in second step, the samples were pressed with 60 % (F60) of the machine's energy, which means a kinetic energy of 10200 J. In third step of F30-60-40 process the samples were pressed with 40 % (F40) of the machine's energy, which corresponds to the kinetic energy of 6800 J. At F30-60-80 process, the samples were in third step pressed with 80 % (F80) of the machine's energy, which corresponds to the kinetic energy of 13600 J.

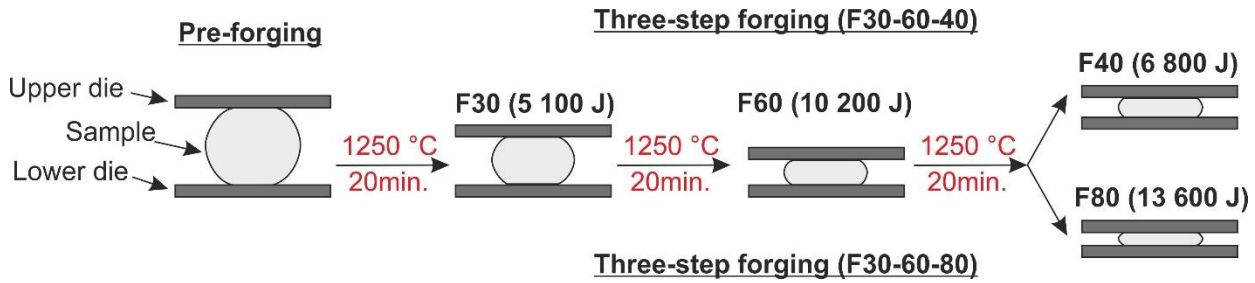

Figure 1 Scheme of forging processes

2.3 Forging simulation

The simulations of F30-60-40 and F30-60-80 forging processes consist of three Transient Thermal Analyses to determine thermal behavior and import temperature values to the structural model and three Transient Structural Analyses, each representing one forging process of a screw press. An initial geometry model of the forming was built as a 3D cylindrical sample with a diameter of 23.8 mm and a length of 65 mm and two dies were modeled as 3D cylinders. Deformed geometry from simulation was used as input geometry in the following simulation. Geometry is the only entry that needs to be transferred, because of the sample being brought up to the high temperatures between individual blows restores its mechanical properties. The sample is being re-meshed in every simulation to replace deformed elements with new tetrahedral elements. The material model consisted of the mechanical properties of as-cast $Al_{0.35}CoCrFeNi$ alloy defined using flow curves characterizing the stress-strain relationship of the material under compression at different strain rates 10^{-2} s^{-1} and 10^{-1} s^{-1} for room temperature and 1 s^{-1} for temperatures in the range from 800 °C to 1200 °C. Top die travel initial speed was set to a speed of 200 mm/s. In the numerical simulation in this work the constant friction law was used with coefficient 0.1 [11]. The loading for this simulation is implemented in the form of kinetic energy equal to the supplied energy of the screw press. The key loading factor is the velocity of the

pressing die. During the experiment of forging, it was possible to determine the velocity of pressing die before impact same as the total duration of forging process. Boundary conditions of structural analysis are the velocity of upper die (according to required energy), fixed lower die, displacement restriction of upper die to be able to move in axial direction only, and imported temperature of the sample. Thermal analysis was used to simulate the sample cooling during its relocation from the furnace to the lower die of the press. It includes three seconds of cooling due to the environmental effects and in the last second the sample is also cooled by the contact with the lower die. Results were imported to the following structural analysis using automatic method. For 3D analysis, deformable hexahedron elements with a size of 2.5 mm and 15 mm were used to mesh the initial cylindrical sample and dies, respectively.

2.4 Microstructure characterization

The chemical and phase composition of the as-cast alloy was measured by energy-dispersive X-ray spectrometry (EDS). The microstructure of the alloy was studied by stereo microscopy (SM) using Carl Zeiss SteREO Discovery V20 microscope. Standard metallographic techniques, including grinding on SiC papers from 60 to 2000 (grains/cm^2) and polishing with diamond suspensions from 6 to 0.3 μm particle size, were applied. Finally, the surfaces were electropolished at 5 V at the temperature of -20 °C using an electrolyte composed of 70 % ethanol, 20 % glycerine and 10 % perchloric acid (in vol%). The grain size was measured on SM micrographs using a computerized image analyzer equipped with the software SigmaScan Pro. The grain size was evaluated as the median value of the ferret diameter. The achieved data were treated statistically.

3. RESULTS AND DISCUSSION

3.1 Material characterization

Figure 2 shows the average chemical composition of the studied $Al_{0.35}CoCrFeNi$ alloy measured by EDS. The alloy is composed of solid solution with FCC structure [11]. **Figure 3** shows pre-forged shape of sample after forging at room temperature with 25 % of machine energy. The microstructure was evaluated by a median values of grain: (i) size 1191 μm, (ii) major length 1840 μm and (iii) minor length of 876 μm. No cracks were observed in the alloy after HT or pre-forging.

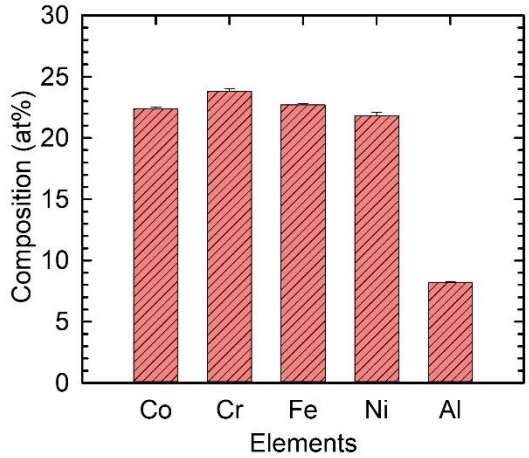

Figure 2 EDS analysis of $Al_{0.35}CoCrFeNi$ alloy (in at%)

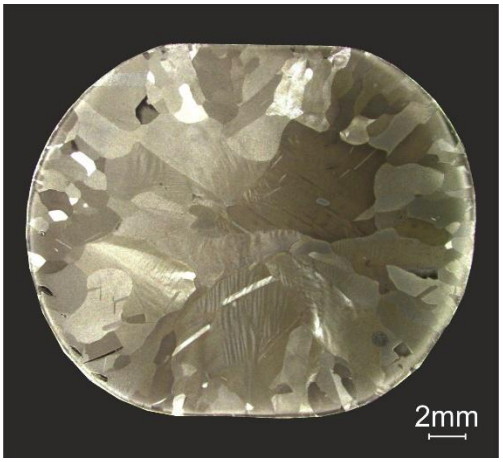

Figure 3 Grain structure of pre-forged sample

3.2 Numerical simulation and microstructure evaluation after forging

The numerical simulation allowed modeling the distribution of the equivalent plastic strains on the cross section of the samples after each forging step. The equivalent plastic strain was separately evaluated in the two regions: region I – in the middle of the sample, region II – in the barreled parts of the sample as is marked in the **Figure 4**. **Figures 4 (a)** and **4(b)** show the results of equivalent plastic strain on the cross section of the sample after F40 and F80 forging. An almost uniform distribution of equivalent plastic strain was observed across the specimens after both forgings. The distribution after F40 forging decrease gradually from the highest values of 0.26 in the middle of the sample to 0.07 in the barreled parts of the sample. After F80 forging, the differences in values are much higher and while in the middle the values reached from 0.59 to 0.40, in the barreled parts of the sample were 0.17.

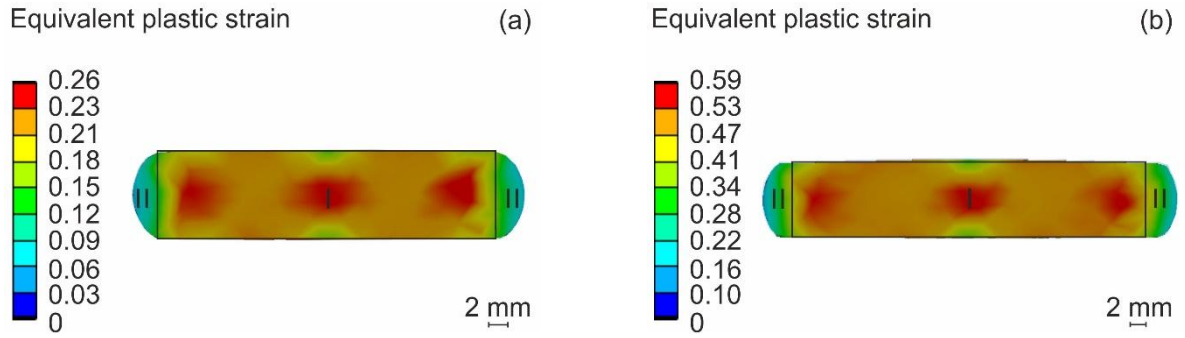

Figure 4 Results of equivalent plastic strain on the cross section of the samples after (a) F40 and (b) F80 forging

Figures 5 show the microstructure of the samples after F40 and F80 forging in the middle (region I) and the barreled parts (region II) of the samples. The grain structure after F40 forging in regions I and II is shown in the **Figures 5(a)** and **5(b)**, respectively. After F40 forging, the microstructure of the sample had a uniform distribution of dynamically recrystallized equiaxed grains with a measured median grain size of 64 ± 1 μm in the region I (**Figure 5(a)**) and the area fraction of 97 %. **Figure 5(b)** shows grain structure in region II with measured median grain size of 75 ± 6 μm and the area fraction of the recrystallized grains of 85 %. The grain structure after F80 forging in regions I and II is shown in the **Figures 5(c)** and **5(d)**, respectively. A high values of the equivalent plastic strain in the region I lead to the microstructure with duplex size of grains. Along the larger grains with a median grain size of 86 ± 3 μm, colonies of small dynamic recrystallized grains with a median grain size of 23 ± 1 μm, were formed in region I (**Figure 5(c)**) with an area fraction of 69 %. Dynamically recrystallized equiaxed grains with a median grain size of 45 ± 5 μm were formed in the region II (**Figure 5(d)**). Their area fraction was estimated to be 95 %.

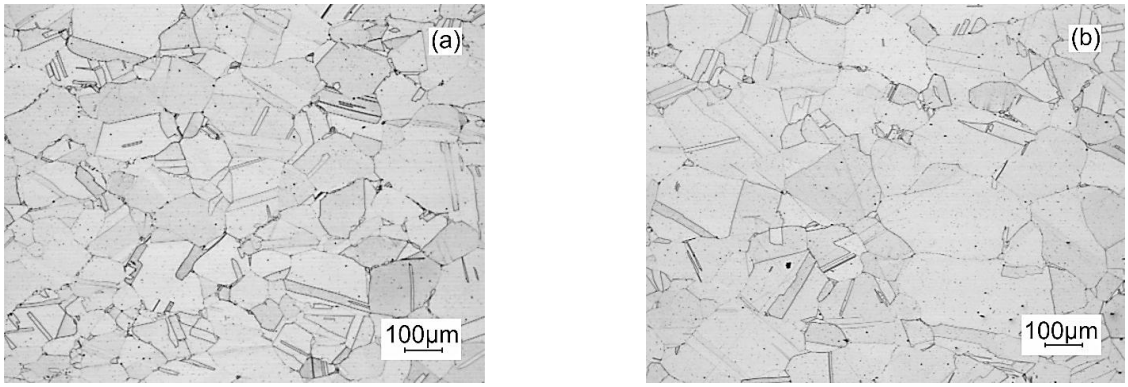

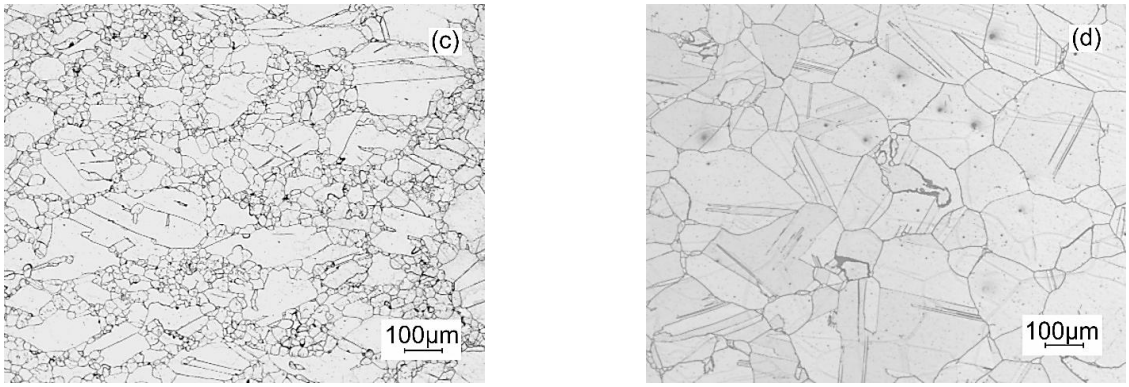

Figure 5 Cross sections of forged samples with a grain structure after F40 forging in regions (a) I (b) II and after F80 forging in regions (c) I and (d) II

Finite element analysis allowed us to simulate the influence of temperature, equivalent stress, and equivalent plastic strain in the F40 and F80 forged samples, which affect the formation of dynamically recrystallized grains as shown in **Figures 6(a)** and **6(b)**, respectively. After F40 forging, region I was formed with a length of approximately 36 mm and corresponding measured median grain size of d = 64 ± 1 μm, as shown in **Figure 6(a)**. In this region I, was a small decrease in the equivalent stress from 580 MPa to 520 MPa, equivalent plastic strain from 26 % to 23 %, and temperature from 1220 °C to 1208 °C. In region II, there was a decrease in equivalent stress from 520 MPa to 280 MPa, equivalent plastic strain from 23 % to 7 %, and temperature from 1208 °C to 1178 °C. The measured median grain size of d = 75 ± 6 μm in this region II after F40 forging slightly increased in comparison with region I. As shown in **Figure 6(b)**, after F80 forging, the region I was formed with a length of approximately 38 mm and with duplex size of grains corresponding to a measured median grain size of larger grains of d_L = 86 ± 3 μm and small grains of d_S = 23 ± 1 μm. This could be due to high values of uniformly distributed equivalent stress around 815 MPa, equivalent plastic strain with values ranging from 59 % to 40 % and temperature from 1213 °C to 1190 °C in region I. In region II, a decrease in equivalent stress from 800 MPa to 385 MPa, equivalent plastic strain from 40 % to 17 %, and temperature from 1190 °C to 1173 °C was observed.

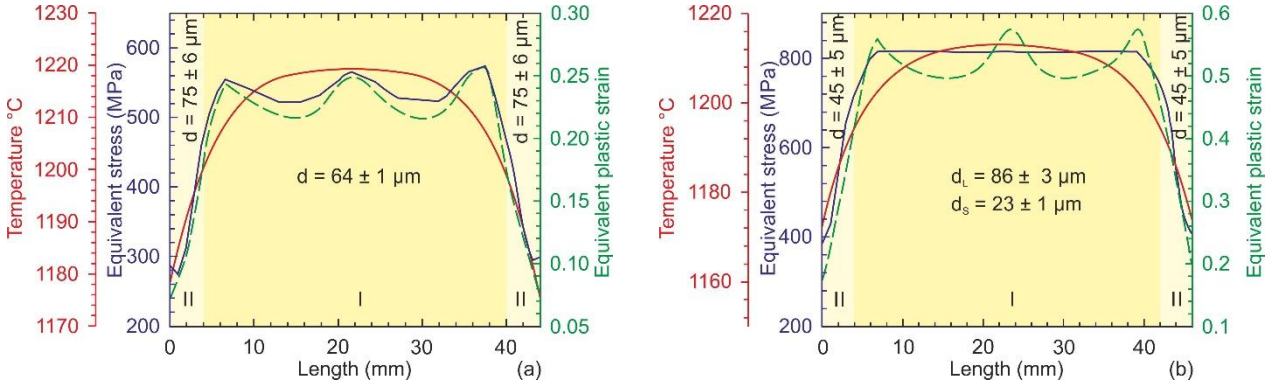

Figure 6 Dependence of temperature, equivalent stress and equivalent plastic strain along the cross section of the sample after: (a) F40 and (b) F80 hot forging

4. CONCLUSION

The F30-60-40 and F30-60-80 three-step hot forging processes were investigated by numerical simulation and microstructure evaluation in the $Al_{0.35}$CoCrFeNi high entropy alloy. The following conclusions can be concluded:

1) The high entropy alloy retained its face-centered cubic (FCC) structure, with no phase transformations observed during hot forging processes.
2) The finite element analysis successfully predicted regions where dynamically recrystallized grains formed using the distribution of equivalent plastic strain. Proposed processes were applied to the alloy and experimentally verified.
3) The final forging step F40 of F30-60-40 process, effectively unified grain size and achieved a uniform grain structure throughout the sample.
4) Both forging processes were experimentally applied and validated, confirming the effectiveness of the simulations and supporting the potential for process optimization in high entropy alloys.

ACKNOWLEDGEMENTS

This publication was created as part of the solution to the grant project "Resistance of wrought complex concentrated alloys to hydrogen embrittlement" of the SAS Return Project Scheme and funded by the Slovak Research and Development Agency under the contract APVV-23-0206 and Slovak Grant Agency for Science under the contract VEGA 2/0018/22. The work was also funded by the EU NextGenerationEU through the Recovery and Resilience Plan for Slovakia under the project No. 09I04-03-V02-00005.

REFERENCES

[1] YEH, J. W., CHEN, S.K., LIN, S.J., GAN, J.Y., CHIN, T.S., SHUN, T.T., TSAU, C.H., CHANG, S.Y. Nanostructured high-entropy alloys with multiple principal elements: Novel alloy design concepts and outcomes. *Advanced Engineering Materials*. 2004, vol. 6, no. 5, pp. 298-302.

[2] LI, W., XIE, D., LI, D., ZHANG, Y., GAO, Y., LIAW, P.K. Mechanical behavior of high-entropy alloys. *Progress in Materials Science.* 2021, vol.118, pp. 100777.

[3] WANG, X., ZHANG, Z., WANG, Z., REN, X. Excellent tensile property and its mechanism in Al0.3CoCrFeNi high-entropy alloy via thermo-mechanical treatment. *Journal of Alloys and Compounds.* 2022, vol. 897, pp.163218.

[4] HAGHDADI, N., PRIMIG, S., ANNASAMY, M., CIZEK, P., HODGSON P.D., FABIJANIC, D.M. On the hot-worked microstructure of a face-centered cubic Al0.3CoCrFeNi high entropy alloy. *Scripta Materialia.* 2020, vol. 178, pp.144–9.

[5] PRASAD, N., BIBHANSHU, N., NAYAN, N., AVADHANI G.S., SUWAS S. Hot deformation behavior of the high-entropy alloy CoCuFeMnNi. *Journal of Materials Research.* 2019, vol. 34, pp. 744–55.

[6] CHEN, F., CUI, Z., CHEN, J. Prediction of microstructural evolution during hot forging. *Manufacturing Review.* 2014, vol. 1, no. 6, pp. 1-21.

[7] BUCKINGHAM, R.C., ARGYRAKIS, C., HARDY, M.C., BIROSCA, S. The effect of strain distribution on microstructural developments during forging in a newly developed nickel base superalloy. *Materials Science & Engineering A*. 2016, vol. 654, pp. 317–328.

[8] SHABANI, A., TOROGHINEJAD, M.R., AMINAEI, M., CAVALIERE, P. Dynamic recrystallization nanoarchitectonics of FeCrCuMnNi multi-phase high entropy alloy. *Journal of Alloys and Compounds*. 2023, vol. 968, pp. 172001.

[9] CHEN, S., QIN, Y. Comparison study of multistep forging and injection forging of automobile fasteners. *MATEC Web of Conferences.* 2015, vol. 21, pp. 1–7.

[10] CHEN, S., QIN, Y., CHEN, J.G., CHOY, C.M. A forging method for reducing process steps in the forming of automotive fasteners. *International Journal of Mechanical Sciences*. 2018, vol. 137, pp. 1–14.

[11] ŠTAMBORSKÁ, M., PELACHOVÁ, T., DANKO, D., OROVČÍK, L. Influence of hot forging on grain formation in Al0.35CoCrFeNi high-entropy alloy: numerical simulation, microstructure and mechanical properties. *Archives of Civil and Mechanical Engineering*. 2024, vol. 24, pp. 241.